Metalloenzyme-like catalyzed isomerizations of sugars by Lewis acid zeolites

Ricardo Bermejo-Deval[a], Rajeev S. Assary[b,c], Eranda Nikolla[a,d], Manuel Moliner[a,e], Yuriy Román-Leshkov[a,f], Son-Jong Hwang[a], Arna Palsdottir[a], Dorothy Silverman[a], Raul F. Lobo[g], Larry A. Curtiss[b], and Mark E. Davis[a,1]

[a]Chemical Engineering, California Institute of Technology, Pasadena, CA 91125; [b]Materials Science Division, Argonne National Laboratory, Argonne, IL 60439; [c]Chemical and Biological Engineering, Northwestern University, Evanston, IL 60228; [d]Chemical Engineering and Materials Science, Wayne State University, Detroit, MI 48202; [e]Instituto de Tecnología Química, UPV-CSIC, Universidad Politécnica de Valencia, Consejo Superior de Investigaciones Científicas, 46022 Valencia, Spain; [f]Chemical Engineering, Massachusetts Institute of Technology, Cambridge, MA 02139; and [g]Center for Catalytic Science and Technology, Chemical Engineering, University of Delaware, Newark, DE 19716

Contributed by Mark E. Davis, April 23, 2012 (sent for review April 4, 2012)

Isomerization of sugars is used in a variety of industrially relevant processes and in glycolysis. Here, we show that hydrophobic zeolite beta with framework tin or titanium Lewis acid centers isomerizes sugars, e.g., glucose, via reaction pathways that are analogous to those of metalloenzymes. Specifically, experimental and theoretical investigations reveal that glucose partitions into the zeolite in the pyranose form, ring opens to the acyclic form in the presence of the Lewis acid center, isomerizes into the acyclic form of fructose, and finally ring closes to yield the furanose product. The zeolite catalysts provide processing advantages over metalloenzymes such as an ability to work at higher temperatures and in acidic conditions that allow for the isomerization reaction to be coupled with other important conversions.

glucose isomerization | heterogeneous catalysis | reaction mechanism

There is a growing interest in the use of renewable carbon sources for the production of chemicals, polymers, and fuels. Numerous chemical transformations of biomass into a wide variety of products are currently being explored. We have recently focused on the isomerizations of sugars, and in particular, the isomerization of glucose to fructose (Scheme 1) (1–3), as a key reaction that could be incorporated into a large number of pathways to convert biomass into useful products (4, 5). For example, oligomeric carbohydrates can be depolymerized into glucose monomers that can then be converted to the chemical platform molecule 5-hydroxymethylfurfural (HMF) (4, 5), via the fructose intermediate (3). Analogously, xylose has been converted to furfural via the xylulose intermediate (6). Additionally, the isomerization of glucose to fructose could be a step in creating synthetic glycolysis pathways (7).

We have shown that the isomerization of glucose to fructose can be catalyzed in aqueous media by hydrophobic zeolites that contain Lewis acids (1–3). Specifically, pure-silica zeolites with the zeolite beta structure containing small amounts of framework Ti^{4+} or Sn^{4+}(denoted as Ti-Beta and Sn-Beta, respectively) were able to isomerize glucose to fructose in high yield at relatively low temperatures (383–413 K). The Sn-Beta sample had superior activity to the Ti-Beta material, and could even convert solutions that contained 45 wt% glucose (1). We demonstrated that the reaction mechanism in aqueous media was a true Lewis acid-mediated intramolecular hydride shift (2). Additionally, it was shown that catalyst activity was maintained in aqueous media saturated with sodium chloride and acidic pH. This allowed for the "one pot" conversion of starch to HMF through a cascade reaction sequence involving the homogeneous acid-catalyzed depolymerization of starch to glucose, a heterogeneous Lewis acid-catalyzed isomerization of glucose to fructose, and a homogeneous acid-catalyzed dehydration of fructose to HMF (3).

The activation of molecules containing carbonyl groups, specifically sugars, by solids containing Lewis acid centers is a new area of heterogeneous catalysis. In addition to the isomerization of glucose in aqueous media (1–3), the isomerization of triose sugars in methanol or water (8) and the conversion of sugars to lactic acid derivatives in methanol have been reported using Sn-containing porous solids (9). Activation of carbonyl-containing molecules with solid acids has recently been reviewed, and includes the limited data on solid Lewis acid catalysis (especially in aqueous media) (10).

The conversion of glucose to fructose (used for the production of high-fructose corn syrups) is accomplished commercially by immobilized enzyme catalysts, such as D-xylose isomerase XI. The reaction mechanisms for XI-mediated isomerizations have been investigated because of their relevance to glycolysis and industrial biocatalysis (11). It is well established that the aldose to ketose interconversion occurs by a three-stage mechanism after binding of the cyclic form of glucose takes place. These steps are: (*i*) aldose ring opening to form the acyclic form of the sugar, (*ii*) aldose to ketose isomerization of the linear sugar at C-1 and C-2 via a metal-assisted hydride transfer, and (*iii*) ring closure to release the cyclic form of the ketose (see Scheme 1). Similarly, it has been shown that this metalloenzyme requires two divalent metal ions (M1 and M2) for the enzyme to be active. The preferred metal ions are Mg^{2+} or Mn^{2+}. Only recently, complementary X-ray and neutron diffraction techniques aimed at probing the location and dynamics of H/D atoms in XI crystal structures have been exploited to reveal important details of the enzyme reaction mechanism (12). Three important new features were elucidated: (*i*) the primary role of M1 (in conjunction with specific amino acid residues) is to destabilize the pyranose structure and promote the ring opening of the sugar, (*ii*) M2 binds and stabilizes O1 and O2 on the acyclic sugar, promoting the hydride shift from C2 to C1, and (*iii*) a hydroxyl group bound to M2 is responsible for the deprotonation/protonation sequences that shuttle protons involved in the interconversion of aldehydes and hydroxyl groups between O2 and O1.

Sn-Beta and Ti-Beta reveal a number of analogous reaction patterns to metalloenzymes when isomerizing glucose. In addition to having high activity and selectivity similar to the metalloenzyme (1), Sn-Beta was demonstrated to perform the isomerization via a metal-assisted intramolecular hydride shift (2). Given the potential significance of this emerging area of heterogeneous catalysis and the possibilities of drawing analogies between enzyme and heterogeneous catalysis, it is important to understand the molecular details of the reaction pathways using these solids. Here, we investigate the glucose isomerization reac-

Author contributions: R.B.-D., R.S.A., Y.R.-L., R.F.L., L.A.C., and M.E.D. designed research; R.B.-D., R.S.A., E.N., M.M., S.-J.H., A.P., and D.S. performed research; R.B.-D., R.S.A., Y.R.-L., S.-J.H., R.F.L., L.A.C., and M.E.D. analyzed data; and R.B.-D., R.S.A., Y.R.-L., L.A.C., and M.E.D. wrote the paper.

The authors declare no conflict of interest.

Freely available online through the PNAS open access option.

[1]To whom correspondence should be addressed. E-mail: mdavis@cheme.caltech.edu.

This article contains supporting information online at www.pnas.org/lookup/suppl/doi:10.1073/pnas.1206708109/-/DCSupplemental.

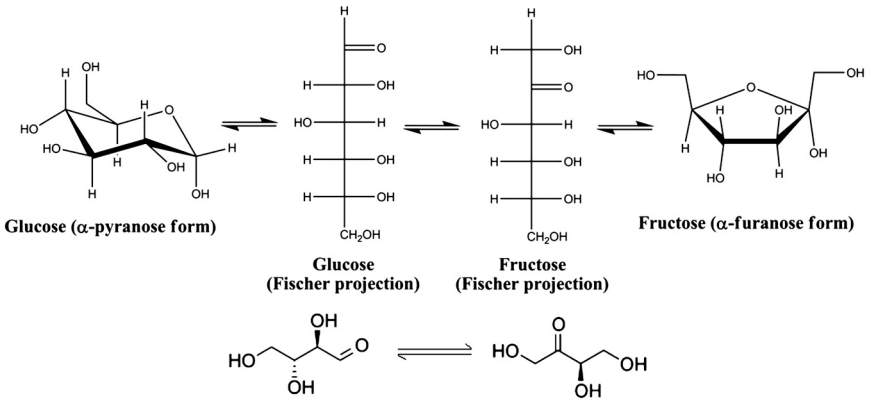

Scheme 1. Schematic representations of the isomerization of glucose to fructose (*Top*) and erythrose to erythrulose (*Bottom*).

tion catalyzed by hydrophobic zeolites that contain Lewis acid centers using a number of experimental and theoretical techniques. The goal is to clarify the sequence of bond breaking and bond forming events in the reaction pathway by using a combination of experimental and theoretical methods, and to determine if there are further similarities between the heterogeneous, Lewis acid catalysts, and the metalloenzyme pathways.

Results and Discussion

Reaction Pathways for Glucose Isomerization on Sn-Beta. ***Ring opening step.*** The initial step in the enzymatic isomerization of glucose to fructose involves the ring opening of a glucose molecule at M1 (12). To determine if a similar pathway is followed by Sn-Beta, the adsorption of ^{13}C labeled glucose and fructose into Sn-Beta and Si-Beta (pure-silica zeolite without Lewis acid active sites: used as control) was investigated using ^{13}C NMR (see Fig. 1). Spectra obtained from glucose and fructose adsorbed into Si-Beta show that the sugars are in their cyclic configurations (resonances between 100 and 90 ppm are assigned to the alpha and beta anomers of the pyranose and furanose rings). No new resonances are observed when compared to the spectra of pure glucose or fructose solutions. Conversely, upon adsorption of these sugars in Sn-Beta, new resonances at ca. 30, 130, 180, and 214 ppm appear. The resonance at 214 ppm is at the chemical shift reported for the keto carbonyl carbon of the acyclic form of fructose (13). Cross polarization (CP) experiments with variable contact times are consistent with an assignment of a keto group for the 214 ppm resonance (Fig. 1). The CP method is based on ^{1}H-^{13}C heteronuclear dipolar coupling so the ^{13}C signal strongly depends on their internuclear distance. Appearance of the 214 ppm resonance only at longer contact times (0.1 and 1.0 ms) rules out the possibility of the carbonyl carbon having a C–H bond as in an aldehyde. Quantitative NMR measurements performed on adsorbed fructose samples reveal that the amount of the acyclic form is on the same order of magnitude as the amount of Sn present in the sample. Because of the errors in the elemental analyses and NMR experiments, greater precision on the estimate of the amount of the acyclic form is not possible. These measurements indicate that ca. 5% of the fructose inside of the zeolite is in the acyclic form, approximately an order of magnitude larger than in solution. Additionally, when fructose is adsorbed in Sn-Beta (but not in Si-Beta), IR measurements reveal the presence of a carbonyl band at ca. 1728 cm^{-1} that has been assigned previously to the keto carbonyl of the acyclic form of fructose (14) (*SI Appendix*, Fig. S1). Altogether, these data provide direct evidence for the presence of ring opened fructose molecules in Sn-Beta, show that Sn is necessary to observe the acyclic form of fructose, and also suggest that Sn plays an important role in stabilizing the acyclic form of fructose.

The acyclic form of glucose contains an aldehyde with a chemical shift around 205 ppm (15). This resonance is not observed in the glucose adsorption experiments. Certainly, if the acyclic forms of glucose and fructose were present in similar proportions as measured in solution, acyclic glucose would be about a hundred times lower in concentration than acyclic fructose and could not be detected by solid-state NMR (16). Note that the 214 ppm resonance is present in the sample where glucose is adsorbed into Sn-Beta in an amount that corresponds to approximately 30% of the amount observed in the fructose adsorption experiment (*SI Appendix*, Fig. S2). The existence of this resonance implies that some of the glucose has ring opened and isomerized to the ring open form of fructose. In fact, when this sample was reanalyzed after several months of storage at room temperature, the reaction proceeded further. These NMR data strongly support the ring opening reaction pathway illustrated in Scheme 1. While there is an IR assignment of the keto carbonyl of the acyclic form of fructose, no assignment for the acyclic aldehyde carbonyl of glucose has been reported. However, when glucose is adsorbed on Sn-Beta, (but not Si-Beta) there is a broad band at ca. 1730–1720 cm^{-1} that is reasonable to assign to the combination of

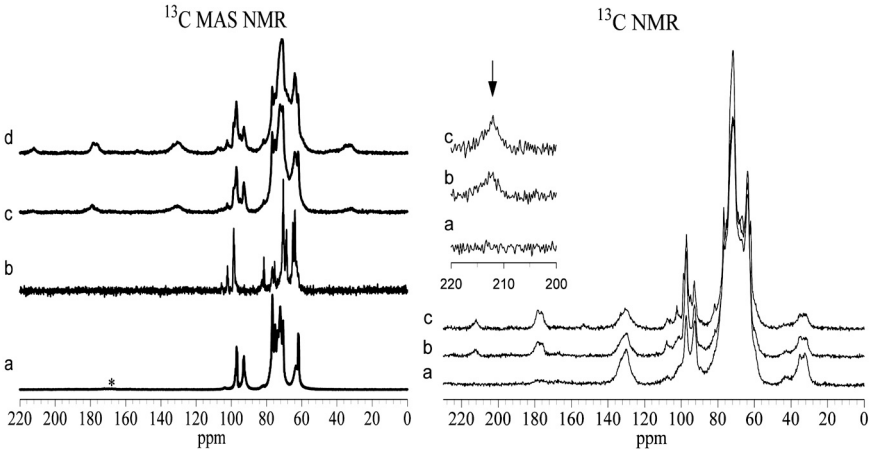

Fig. 1. ^{13}C Solid State NMR of sugars adsorbed in zeolites. (*Left*) (*A*) glucose adsorbed into Si-Beta, (*B*) fructose adsorbed into Si-Beta, (*C*) glucose adsorbed into Sn-Beta, (*D*) fructose adsorbed into Sn-Beta. (*Right*) spectra from fructose adsorbed into Sn-Beta, (*A*) cross polarization contact time of 0.1 ms, (*B*) cross polarization contact time of 1.0 ms, and (*C*) no cross polarization.

the 1728 cm^{-1} band from the acyclic fructose and a band from the aldehyde carbonyl (ca. 1720 cm^{-1}) of the acyclic glucose (*SI Appendix*, Fig. S1). These band intensities and assignments are consistent with the ^{13}C NMR results. Overall, the NMR and IR data from both the glucose and fructose adsorbed in Sn-Beta imply that the reaction pathway parallels the reaction steps observed in enzymatic systems.

At this time, we have not assigned the resonances at ca. 30, 130 and 180 ppm in the ^{13}C NMR spectra with Sn-Beta. After reaction with either ^{13}C labeled glucose or fructose, these resonances appear as do others (*SI Appendix*, Fig. S3). The reaction of glucose on either Sn-Beta or Ti-Beta gave ca. 90% yields of glucose, fructose, and mannose (1). From the NMR spectra of the solids after reaction, some of the resonances have been assigned to products that can be observed in solution (*SI Appendix*, Fig. S3, HMF) or remain on the solid and are not observed in solution (*SI Appendix*, Fig. S3, lactic acid). Further attempts to assign the remaining products in solution and on the solids are in progress.

Isomerization step. The enzymatic isomerization step is believed to occur primarily at M2. First, a hydroxyl ion bound to M2 promotes deprotonation at O2 (17). Next, M2 forms a bidentate complex with both O1 and O2, withdrawing electron density from the C–O bonds and effectively polarizing the substrate. This leads to a partial positive character on C1, consequently reducing the energetic barrier for hydride shift. Finally, the protonated hydroxyl group at M2 donates the proton to O1, converting the aldehyde into a hydroxyl group. Kinetic studies on enzymatic systems suggest that the kinetically limiting factor is the hydride shift. Interestingly, a similar conclusion can be drawn for isomerizations catalyzed by Sn-Beta and Ti-Beta. Previously, we showed that the mechanism of the glucose isomerization reaction using Sn-Beta involves a Lewis acid-mediated intramolecular hydride shift (2). A kinetic isotope effect of ca. 2 for both Sn-Beta (2) and Ti-Beta is observed using glucose labeled with deuterium at the C2 position, and is consistent with the theoretical kinetic isotope effect calculated using the Lewis acid-mediated intramolecular hydride transfer as the rate-determining step (*SI Appendix*, Text S1). Activation energies obtained from initial rate data of glucose to fructose isomerization are 21.2 ± 0.7 kcal/mol (343–373 K) and 37.1 ± 1.0 kcal/mol (388–403 K) for Sn-Beta and Ti-Beta, respectively. These data show that the hydride step is kinetically relevant and that Sn-Beta is a more active catalyst than Ti-Beta at the reaction conditions used.

Reaction Centers with Sn or Ti Containing Zeolites. The reaction pathway over Sn-Beta and Ti-Beta proceeds via a ring opening, hydride shift, and a ring closing mechanism. To gain further insights into how these conversions proceed at the metal centers, the state of the Sn in the zeolite was investigated by solid-state NMR methods. Different atomic arrangements of framework Sn are depicted in Scheme 2. Framework Sn can exist in two different states, octahedral or tetrahedral, depending if is hexacoordinated or tetracoordinated. Also, Boronat et al. (18) proposed that

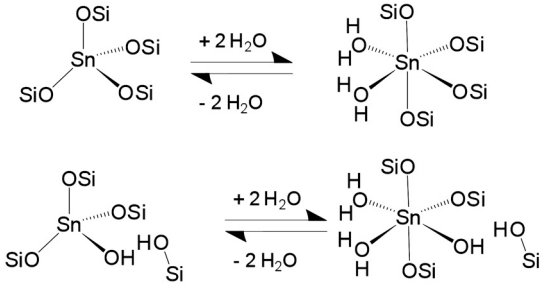

Scheme 2. Schematic representations of the closed (*Top*) and open (*Bottom*) sites in Sn-Beta. *Left*: dehydrated (tetrahedral), *Right*: hydrated (octahedral).

framework Sn can be located in two different types of sites, closed or open, depending if the Sn centers have four bonds to the silicon atoms of the zeolite framework through bridging oxygens or if the Sn centers have three such bonds to the framework and one bond that has been hydrolyzed to produce Sn-OH and an adjacent silanol group (Si-OH). These atomic arrangements are analogous to those proposed for Ti in Ti-Beta and Ti in pure-silica ZSM-5 (called TS-1) (ref. 19 and references therein). For the case of Ti, no NMR data are available; however, EXAFS data provide strong evidence for the open site (19). Additionally, IR spectra can be used to identify the silanol group adjacent to the Ti center in the open site.

^{119}Sn solid-state NMR studies of the Sn-Beta prepared with ^{119}Sn enriched starting materials are shown in Fig. 2. After calcination to remove the structure directing agent (SDA) and exposure to ambient conditions, the NMR spectrum reveals the presence of octahedral Sn (main resonances at ca. −685 and −700 ppm; Fig. 2 *A* and *B*). Upon heating to 393 K under vacuum, water is removed and the dehydrated spectrum shows the presence of tetrahedral Sn (main resonances at ca. −420 to −443 ppm; Fig. 2 *A* and *B*). Reexposure to ambient conditions returns the sample to a state with octahedral Sn (shown in Fig. 2*A* and also occurs with the sample show in Fig. 2*B*). The calcination conditions affect the spectra that are obtained after dehydration, thus suggesting that the ratio of the −420 ppm resonance to −443 ppm resonance can vary with the pretreatment conditions (compare Fig. 2 *A* to *B*).

Corma et al. have shown that hydrated Sn-Beta has octahedral Sn while dehydration can change the Sn coordination to tetrahedral (20). Corma et al. reported only one resonance in their dehydrated sample, while our results show that there are two main resonances, i.e., the tetrahedral Sn centers. These results could be due to differences in calcination conditions. Using diffuse reflectance UV–Vis (1, 20), we confirmed that Sn remains within the framework of the zeolite. Our cross-polarized NMR spectra with variable contact time (Fig. 2*C*) show that only one of the Sn environments has a proton source in its neighborhood. Based on the fact that the Sn atoms are located in the zeolite framework, we assign the resonances in our NMR spectra to the open (−420 ppm) and closed (−443 ppm) arrangements for dehydrated Sn-Beta. Upon hydration, these tetrahedral Sn centers coordinate two additional water molecules to become octahedral (Scheme 2). Thus, the Sn-Beta, and by analogy Ti-Beta, will have both open and closed sites that may be active reaction centers.

Khouw and Davis showed that the active site for the oxidation of alkanes using aqueous hydrogen peroxide with TS-1 was the open Ti site (also required the presence of the adjacent silanol group for reactivity to occur) (21). After exchanging the proton on the adjacent silanol group of the Ti center with Na^+ [verified by IR, band is in the 985–960 cm^{-1} region of the spectrum (21)], the catalytic activity was completely eliminated. Repopulation of the silanol group with proton recovered the catalytic active to conclusively show for this reaction that the active site was the open site alone. Boronat et al. used theoretical calculations to suggest that acetonitrile gives two IR bands when adsorbed on the open and closed sites of Sn-Beta (18). By correlating the intensity of the IR band assigned to the acetonitrile adsorbed on the open site (as a measure of the amount of the open site) to the initial catalytic activity of the Baeyer–Villiger oxidation of cyclic ketones, these workers concluded that the open Sn site was the active center for this reaction.

TS-1 is not active for the isomerization of glucose; however, this most likely occurs because glucose (kinetic diameter ca. 0.8 nm) is too large to diffuse into the pores of this zeolite (pore diameter ca. 0.55 nm) (1). To test this hypothesis, the isomerization of erythrose to erythrulose was employed as a test reaction that uses a reactant that could diffuse into the pores of TS-1. TS-1 is active for the isomerization of erythrose, and these results support the premise that glucose diffuses into the zeolite catalysts in

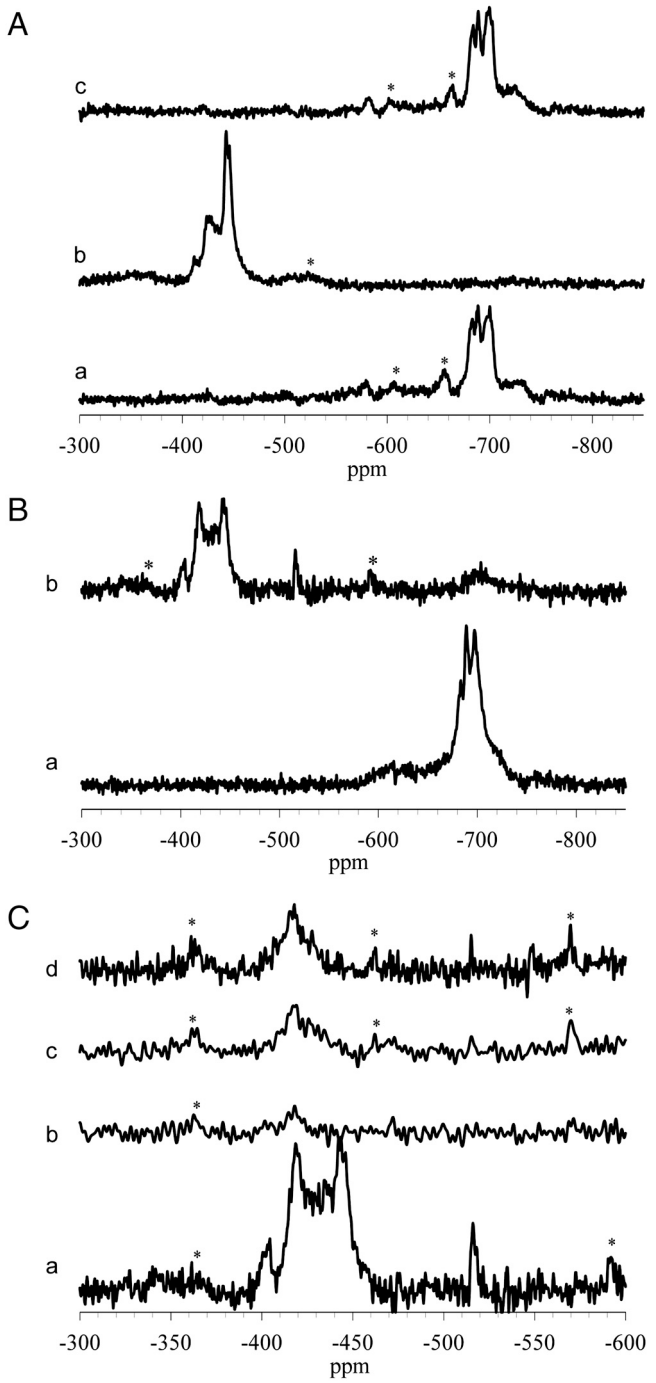

Fig. 2. ^{119}Sn Solid State NMR spectra of Sn-Beta. *A*. ^{119}Sn Solid State NMR spectra of Sn-Beta after different treatments. (*a*) calcined, (*b*) dehydrated after calcination, (*c*) rehydrated after step (*b*). The spinning rate was 14 kHz and spinning sidebands are marked by *. *B*:^{119}Sn MAS NMR spectra of Sn-Beta as a function of hydration. (*a*) Sample was calcined with more humid conditions and exposed to ambient conditions, and (*b*) sample shown in (*a*) after vacuum drying at 393 K. The spinning rate was 14 kHz and spinning sidebands are marked by *. *C*: ^{119}Sn MAS (*a*) and CPMAS NMR (*b*–*d*) spectra for dehydrated Sn-Beta. The cross polarization contact times from ^{1}H to ^{119}Sn were varied: *b*) 0.2 ms, *c*) 1.0 ms, *d*) 2.0 ms. The spinning rate was 14 kHz for the MAS spectrum and 10 kHz for the CPMAS spectra, and spinning sidebands are marked by *.

the ring-closed (pyranose) form, and that the ring-closed form is too large to diffuse into TS-1. Since TS-1 is active for the isomerization of erythrose, this reaction can be used to test whether or not exchanging the proton on the adjacent silanol group of the Ti center with Na^+ affects the isomerization activity like it did with the oxidation reaction.

Following the work by Khouw and Davis, TS-1, Ti-Beta, and Sn-Beta were exchanged with Na^+ to identify which type of Sn or Ti center is active for the isomerization reactions. The presence of the sodium atom was confirmed by IR spectroscopy (21). TS-1 catalyzed the isomerization of erythrose to erythrulose independent of whether or not the adjacent silanol group of the Ti center was exchanged with Na^+ [unlike the oxidation reaction (21)]. Ti-Beta and Sn-Beta were also active for the isomerization of erythrose reaction. Additionally, Ti-Beta and Sn-Beta were also active for the isomerization of both erythrose and glucose before and after Na^+ exchange. In order to rule out the possibility that the Na^+ was being removed from the adjacent silanol group during the reactions in pure water solvent [the oxidation reaction with TS-1 was conducted in a mixed methanol/water solvent (21)], the glucose isomerization reaction was performed in saturated NaCl solutions. We have shown previously that the glucose isomerization reaction can proceed at these conditions (3). After reaction, the IR spectrum of the Sn-Beta shows that the adjacent silanol group remained populated with Na^+. These reaction data, when taken in total, do not allow us to distinguish whether the open site or the closed site (or both) is the active center. It is possible that the open site is an active site, but the adjacent silanol group, whether in the proton or sodium form, does not significantly alter the reaction rate (unlike the case with TS-1 and the oxidation reaction).

To further investigate the nature of the active Sn site, Sn-containing zeolite beta was prepared using trichloromethyltin as the Sn source (*SI Appendix*, denoted as CH_3Sn-Beta, powder X-ray diffraction pattern in Fig. S4). Successful preparation of zeolite beta with framework tin in this case gives tin centers that exclusively have three bonds via oxygen atoms to framework silicon atoms. The SDA in this sample is removed by acid extraction rather than calcination to preserve the Sn-CH_3 bond. ^{13}C MAS NMR and thermogravimetric analyses before and after extraction can be used to demonstrate that the extracted CH_3Sn-Beta sample does not contain a significant amount of SDA. In addition, N_2 adsorption experiments performed on the extracted CH_3Sn-Beta and on a calcined pure-silica Beta (Si-Beta) samples show that both materials have nearly identical adsorption isotherms and equivalent micropore volumes, thus further confirming that there is little to no SDA occluded within the pores after the acid treatment (*SI Appendix*, Fig. S5). Glucose isomerization reactions performed in the presence of the extracted CH_3Sn-Beta give negligible glucose conversion after 45 min at 110 °C (*SI Appendix*, Fig. S6). In contrast, reactions performed with Sn-Beta show nearly 50% conversion at the same reaction conditions. Calcination of CH_3Sn-Beta provides an active glucose isomerization catalyst that was no different from the Sn-Beta samples prepared from tin tetrachloride (*SI Appendix*, Fig. S6). The similar reactivity of these two samples suggests that the amounts of both the open and closed sites are predominantly a function of the high temperature calcination conditions (upon loss of the methyl group the tin center would have an OH group that could then condense with the adjacent silanol group to give a closed site for some of the tin centers in CH_3Sn-Beta).

In an attempt to alter the distribution of the Sn sites, the CH_3Sn-Beta was first exchanged into the sodium form and then calcined (attempt to limit condensation by reducing the number of available silanol groups adjacent to the open Sn center). The reaction rates for this sample were virtually identical to those obtained with the non-exchanged sample. Based upon these results alone, it cannot be established which site is the active site or whether both sites are active. These results strongly suggest that the calcination and initial exposure to the reaction environment interconverts the distribution of the tin centers between the open and closed sites, bringing them to an equilibrated state dictated by the reactions conditions. Alternatively, the reactivity of the two

types of sites could be the same, but this situation is highly unlikely. This hypothesis implies that the distribution of open and closed sites is dynamic at reaction conditions, requiring the development of an in-situ method for determining site distributions. Such a characterization technique is currently not available to us, and thus theoretical studies were used to gain further insights into the structure and reactivity of the active site.

Computational Studies for Glucose–Fructose Isomerization. Quantum chemical studies were performed to gain further molecular-level understanding of the glucose–fructose isomerization pathways and to compare with experimental kinetics of both Sn-Beta and Ti-Beta. The structures and energies of intermediates and transition states were determined (*SI Appendix*, Text S2). Based on previous experimental and theoretical studies, it has been suggested that the open site in Sn-Beta, TS-1, and Ti-Beta is the active site for reactions other than the glucose isomerization (18, 19, 21, 22). The enthalpy profile (Fig. 3) and the free energy profile (*SI Appendix*, Fig. S7 and Text S3) for glucose–fructose isomerization catalyzed by the Sn-Beta open site indicate that, similarly to enzymatic systems, the process can be described as a sequence of ring opening (I to IV), hydride shift (V to VI), and ring closing (VI to IX) events. The initial adsorption of cyclic glucose and ring opening does not require any apparent reaction barriers. The process requiring significant activation is the intra molecular hydride shift (V to VI) via a transition state (V^{TS}), and is consistent with experimental results showing a kinetic isotope effect when the glucose is labeled with deuterium at the C2 position.

The enthalpic profiles for glucose–fructose isomerization catalyzed by three open active site models with and without adjacent silanol groups were also calculated (*SI Appendix*, Fig. S8, Text S4, and Table S1), the activation enthalpy for the glucose–fructose isomerization process was computed to be 18.6, 22.1 and 17.3 kcal/mol for the Sn-Beta open site, the Sn-Beta open site with one silanol group, and Sn-Beta open site with two adjacent silanol groups, respectively. The calculated activation enthalpy for the Sn-Beta open site with one adjacent silanol group is found to be consistent with our experimental value of 21.2 ± 0.7 kcal/mol, and supports the assignment of the catalytic activity to the open site of Sn-Beta for glucose–fructose isomerization. Overall, these calculations show relatively small energetic differences between the three open sites models, thus suggesting that the presence or absence of adjacent silanol groups does not drastically influence reaction rates. This is in agreement with our experimental results showing that catalysts with Na^+ exchanged silanol groups had similar activity as the nonexchanged catalysts.

It was previously shown that the apparent activation energy for the hydride shift associated with the isomerization of glyceraldehyde to dihydroxy acetone is 10 kcal/mol higher for the Sn-Beta closed site than that of an open site (22). The glucose isomerization over the closed site would require the participation of a water molecule to allow for ring opening of the glucose. We have performed calculations on a closed site with the presence of an explicit water molecule and the computed apparent activation barrier is approximately 30 kcal/mol (*SI Appendix*, Text S5 and Fig. S9) and is therefore unlikely to be the primary reaction pathway for glucose isomerization over Sn-Beta. These results support the suggestion that the open site is a catalytically more active site for the glucose–fructose isomerization.

The glucose–fructose isomerization using models of the open sites of Ti-Beta (*SI Appendix*, Scheme S2) was also investigated. The initial glucose absorption on the open Ti-Beta model site (with one silanol group) is much weaker, and the rate limiting hydride shift is 10 kcal/mol higher in barrier height (*SI Appendix*, Figs. S9 and S10 and Text S6) compared to that catalyzed by the open site of Sn-Beta with one adjacent silanol group. This trend is

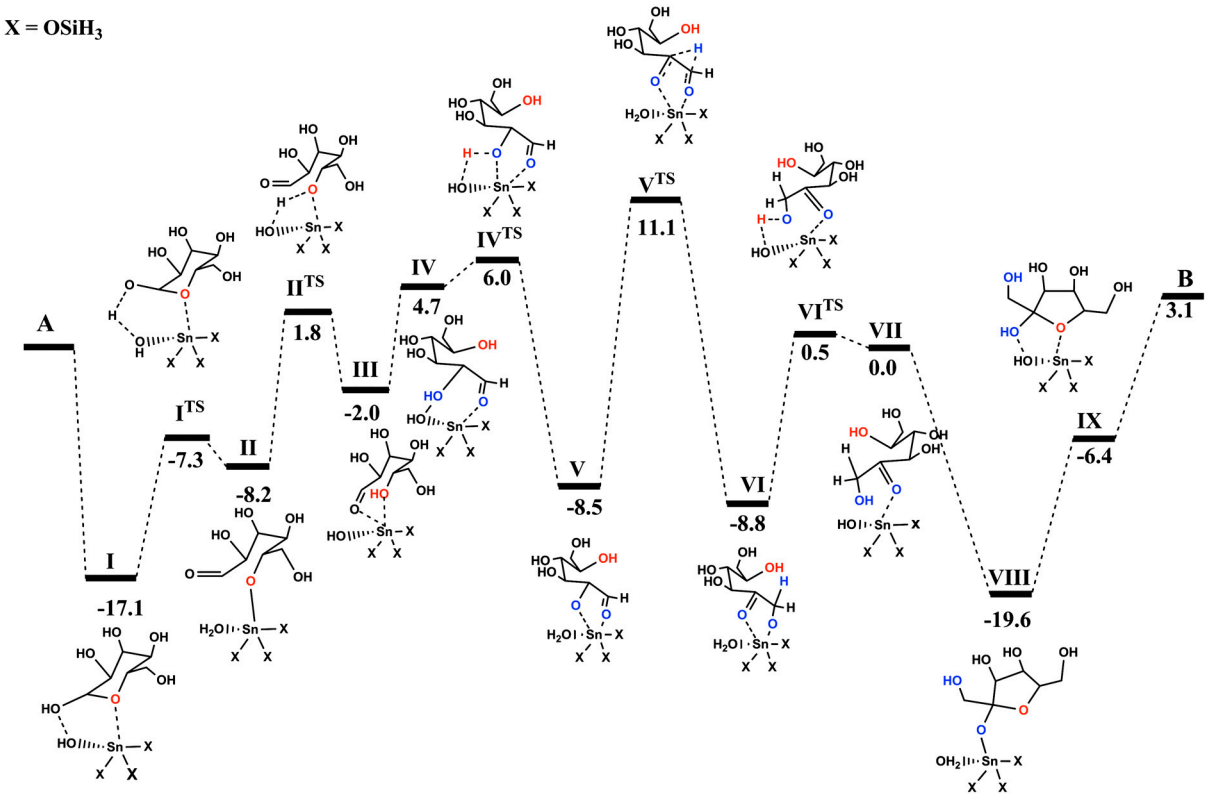

Fig. 3. Computed enthalpy profile (MP2, 298 K in water dielectric) for glucose–fructose isomerization catalyzed by open site of Sn-Beta. The label A denotes the sum of the enthalpy of glucose and the active site model (*SI Appendix*, Scheme S1a) at infinite separation in aqueous medium, B denotes the same quantity for fructose. All energies are relative to the energy of A and are in kcal/mol. Note that the mode of binding of the acyclic glucose to the Sn site is slightly different in structures III and IV.

consistent with previously reported theoretical studies for aldose–ketose isomerization by Sn-Beta and Ti-Beta active site models (22). The computed activation enthalpy for glucose–fructose isomerization catalyzed by the open site of Ti-Beta, open site of Ti-Beta with one adjacent silanol, and the open site of Ti-Beta with two adjacent silanol groups are 28.0, 34.3, and 36.3 kcal/mol, respectively (*SI Appendix*, Table S1). The computed activation enthalpies of Ti-Beta with silanol group(s) are consistent with the experimentally measured activation enthalpy (37.1 ± 1.0 kcal/mol).

Computational results indicate that the acyclic forms of glucose and fructose are equally stabilized by Sn centers (Fig. 3, species V and VI). Gas phase calculations at the G4 level suggest that acyclic fructose is more stable than acyclic glucose by ~2 kcal/mol (ketone groups have more intramolecular hydrogen bonding than the aldehyde) (23). Thus, at thermodynamic equilibrium, cyclic and acyclic species of both sugars (Fig. 3, species I, II, V, VI, VIII, and IX) are expected to be present within the zeolite pores. The enthalpy surfaces support the concept of having acyclic forms strongly coordinated with the Sn active site, which is consistent with the experimental observation of acyclic fructose species by NMR. Note that although the cyclic furanose form of fructose bound to the Sn center has a lower energy (−19 kcal/mol; Fig. 3, species VIII) than the bound acyclic form (−9 kcal/mol; Fig. 3, species VI), it is still possible to observe the bound acyclic form since a barrier of ~10 kcal is required for the cyclization. A similar conclusion can be drawn for glucose.

Conclusions

The metalloenzyme D-xylose isomerase can catalyze the isomerization of glucose to fructose. We previously have shown that Sn-Beta and Ti-Beta can also catalyze this reaction to give similar product distributions to the enzyme, and like the enzyme, Sn-Beta can convert up to 45 wt% aqueous solutions of glucose (1). With Sn-Beta (and to a great extent Ti-Beta), we have shown that the reaction mechanism is very similar to that of the enzyme. We have provided evidence to conclude that the glucose partitions into the zeolite in the cyclic form. In the presence of Sn (or Ti), direct NMR evidence of the acyclic fructose is observed. We infer that acyclic glucose must have first been bound to the Lewis acid center prior to being isomerized to obtain the acyclic fructose. The isomerization is clearly occurring via a Lewis acid-mediated, intramolecular hydride transfer mechanism (2). Here, both experimental results (kinetic isotope effects) and theoretical calculations support the conclusion that the rate-determining step is the intramolecular hydride transfer, and that the open site is likely the active site responsible for isomerization activity. It is exciting to learn that the hydrophobic, Lewis acid containing zeolite catalysts can perform this type of reaction mechanism with glucose and presumably other sugars such as xylose (6) and erythrose. The fact that the zeolite catalysts are quite stable allows them to be used at processing conditions not possible with enzymes, e.g., low pH, high ionic strength, high temperature, and have provided ways of coupling the isomerization reaction to other types of reactions important to the production of chemicals and fuels from biomass (3, 6).

Materials and Methods

Complete details of materials and methods are found in *SI Appendix*.

Synthesis of Materials. The synthesis of the zeolites is described in the *SI Appendix*.

Characterization Methods. Powder X-ray diffraction, solid state NMR, IR an adsorption methods are provided in the *SI Appendix*.

Isomerization Reactions. Details of the experimental methods for the isomerization reactions are given in the *SI Appendix*.

Computational Methods. The methods used for the computational studies are provided in the *SI Appendix*.

ACKNOWLEDGMENTS. The work at Caltech and the University of Delaware was financially supported as part of the Catalysis Center for Energy Innovation, an Energy Frontier Research Center funded by the U.S. Department of Energy, Office of Science, Office of Basic Energy Sciences under Award DE-SC0001004. M.M acknowledges the Fundación Ramón Areces Postdoctoral Research Fellowship Program and the "Subprograma Ramon y Cajal" for Contract RYC-2011-08972 for financial support. R.B.D. acknowledges the Obra Social "la Caixa" for a graduate fellowship. A.P. acknowledges the Caltech Summer Undergraduate Research Fellowship program (SURF) for financial support. The computational studies for this work were supported by the U.S. Department of Energy under Contract DE-AC0206CH11357 and this material is based upon work supported as part of the Institute for Atom-efficient Chemical Transformations (IACT), an Energy Frontier Research Center funded by the U.S. Department of Energy, Office of Science, and Office of Basic Energy Sciences. We gratefully acknowledge grants of computer time from the ANL Laboratory Computing Resource Center (LCRC), and the ANL Center for Nanoscale Materials. This research used resources of the National Energy Research Scientific Computing Center, which is supported by the Office of Sciences of the U.S. Department of Energy under Contract DE-AC02-05CH11231.

1. Moliner M, Román-Leshkov Y, Davis ME (2010) Tin-containing zeolites are highly active catalysts for the isomerization of glucose in water. *Proc Natl Acad Sci USA* 107:6164–6168.
2. Román-Leshkov Y, Moliner M, Labinger JA, Davis ME (2010) Mechanism of glucose isomerization using a solid Lewis acid catalyst in water. *Angew Chem Int Ed Engl* 49:8954–8957.
3. Nikolla E, Román-Leshkov Y, Moliner M, Davis ME (2011) "One-pot" synthesis of 5-(hydroxymethyl)furfural from carbohydrates using tin-beta zeolite. *ACS Catal* 1:408–410.
4. Román-Leshkov Y, Barrett CJ, Liu ZY, Dumesic JA (2007) Production of dimethylfuran for liquid fuels from biomass-derived carbohydrates. *Nature* 447:982–985.
5. Climent MJ, Corma A, Iborra S (2011) Converting carbohydrates to bulk chemicals and fine chemicals over heterogeneous catalysts. *Green Chem* 13:520–540.
6. Choudhary V, Pinar A, Sandler SI, Vlachos DG, Lobo RF (2011) Xylose isomerization to xylulose and its dehydration to furfural in aqueous media. *ACS Catal* 1:1724–1728.
7. Lobo RF (2010) Synthetic glycolysis. *ChemSusChem* 3:1237–1240.
8. Taarning E, et al. (2009) Zeolite-catalyzed isomerization of triose sugars. *ChemSusChem* 2:625–627.
9. Holm MS, Saravanamurugan S, Taarning E (2010) Conversion of sugars to lactic acid derivatives using heterogeneous zeotype catalysts. *Science* 328:602–605.
10. Román-Leshkov Y, Davis ME (2011) Activation of carbonyl-containing molecules with solid Lewis acids in aqueous media. *ACS Catal* 1:1566–1580.
11. Allen KN, et al. (1994) Isotopic exchange plus substrate and inhibition kinetics of D-xylose isomerase do not support a proton-transfer mechanism. *Biochemistry* 33:1481–1487.
12. Kovalevsky AY, et al. (2010) Metal ion roles and the movement of hydrogen during reaction catalyzed by D-xylose isomerase: A joint X-ray and neutron diffraction study. *Structure* 18:688–699.
13. Gouw WJ (1985) Complex isomerization of ketoses: A ^{13}C NMR study of the base-catalyzed ring-opening and ring-closing rates of D-fructose isomers in aqueous solution. *J Am Chem Soc* 107:4320–4327.
14. Yaylayan VA, Ismail AA, Mandeville S (1993) Quantitative determination of the effect of pH and temperature on the keto form of D-fructose by FTIR spectroscopy. *Carbohydr Res* 248:355–360.
15. Drew KN, Zajicek J, Bondo G, Bose B, Serianni AS (1998) ^{13}C-labeled aldopentoses: Detection and quantitation of cyclic and acyclic forms by heteronuclear 1D and 2D NMR spectroscopy. *Carbohydr Res* 307:199–209.
16. Dworkin JP, Miller SL (2000) A kinetic estimate of the free aldehyde content of aldoses. *Carbohydr Res* 329:359–365.
17. Fenn TD, Ringe D, Petsko GA (2004) Xylose isomerase in substrate and inhibitor Michaelis states: Atomic resolution studies of a metal-mediated hydride shift. *Biochemistry* 43:6464–6474.
18. Boronat M, Concepción P, Corma A, Renz M, Valencia S (2005) Determination of the catalytically active oxidation Lewis acid sites in Sn-beta zeolites, and their optimisation by the combination of theoretical and experimental studies. *J Catal* 234:111–118.
19. Bordiga S, Bonino F, Damin A, Lamberti C (2007) Reactivity of TI(IV) species hosted in TS-1 towards H_2O_2-H_2O solutions investigated by *ab initio* cluster and periodic approaches combined with experimental XANES and EXAFS data: A review and new highlights. *Phys Chem Chem Phys* 9:4854–4878.
20. Corma A, Nemeth LT, Renz M, Valencia S (2001) Sn-zeolite beta as a heterogeneous chemoselective catalyst for Baeyer-Villiger oxidations. *Nature* 412:423–425.
21. Khouw CB, Davis ME (1995) Catalytic activity of titanium silicates synthesized in the presence of alkali metal and alkaline earth ions. *J Catal* 151:77–86.
22. Assary RS, Curtiss LA (2011) Theoretical study of 1,2-hydride shift associated with the isomerization of glyceraldehyde to dihydroxy acetone by Lewis acid active site models. *J Phys Chem A* 115:8754–8760.
23. Assary RS, Curtiss LA (2012) Comparison of sugar molecule decomposition through glucose and fructose: A high-level quantum chemical study. *Energy Fuels* 26:1344–1352.

SI Appendix:

Experimental Methods

1. Synthesis of materials

Synthesis of Ti-Beta

Ti-Beta zeolite has been prepared as follows: 7.503 g of tetraethylammonium hydroxide solution (Sigma-Aldrich, 35 wt% in water) was diluted with 15 g of water. Then, 7.016 g of tetraethylorthosilicate (Sigma-Aldrich, 98 wt%) and 0.201 g of titanium (IV) isopropoxide (Sigma-Aldrich, 97%wt) were added to the solution. The mixture was stirred until complete hydrolysis of the tetraethylorthosilicate and titanium (IV) isopropoxide was obtained. Next, the solution was allowed to reach the desired water ratio by complete evaporation of ethanol, isopropanol, and some water. Finally, 0.670 g of HF solution (Mallinckrodt, 48 wt% in water) was added resulting in a thick gel. The gel composition was SiO_2 / 0.021 TiO_2 / 0.54 TEAOH / 0.53 HF / 6.6 H_2O. This gel was transferred to a Teflon-lined stainless steel autoclave and heated at 140°C for 14 days. The solid was recovered by filtration, extensively washed with water, and dried at 100°C overnight. The solid was calcined at 580ºC for 6 hours to remove the organic content located within the crystalline material.

Synthesis of TS-1

TS-1 zeolite was synthesized following the method reported in the patent literature.(*1*) TS-1 was crystallized from a clear solution prepared by mixing titanium butoxide (TNBT, Sigma-Aldrich 97 wt%), tetraethylorthosilicate (TEOS, Sigma-Aldrich 97 wt%), tetrapropylammonium hydroxide (TPAOH, 1M, Sigma-Aldrich) and deionized water. The mixture was stirred until complete hydrolysis of the tetraethylorthosilicate and titanium butoxide was obtained, then allowing complete evaporation of ethanol, butanol and some water until the desired water ratio was reached. The gel composition was SiO_2 / 0.03 TiO_2 / 0.44 TPAOH / 30 H_2O. The TS-1 reaction mixture was charged into Teflon-lined autoclaves and allowed to crystallize at 175ºC for 5 days. The autoclave was rotated at 50 RPM. After cooling, the solid was recovered by filtration, extensively washed with water, and dried at 100°C overnight. The material was calcined at 580ºC for 6 hours to remove the organic content located within the crystalline material.

Synthesis of Sn-Beta, ^{119}Sn-Beta and CH_3-Sn-Beta

Zeolites were prepared as follows: 7.57 g of tetraethylammonium hydroxide solution (Sigma-Aldrich, 35% (w/w) in water) was diluted with 15 g of water. Next, 7.011 g of tetraethylorthosilicate (Sigma-Aldrich, 98% (w/w)) was added, followed by the addition of 0.121 g of tin (IV) chloride pentahydrate (Sigma-Aldrich, 98% (w/w)), 0.121 ^{119}Sn enriched tin(IV) chloride pentahydrate (Cambridge Isotopes, 82% enrichment) or 0.122 g of methyltin trichloride pentahydrate (Sigma Aldrich, 97 wt%), depending if Sn-Beta, ^{119}Sn-Beta, or CH_3-Sn-Beta were synthesized, respectively. The mixture was stirred until complete hydrolysis of the tetraethylorthosilicate was achieved, and then allowed to reach the desired water ratio by complete evaporation of ethanol and some water. Finally, 0.690 g of HF solution (Mallinckrodt, 48% (w/w) in water) was added, resulting in a thick gel. The gel composition was SiO_2 / 0.01 $SnCl_4$ / 0.55 TEAOH / 0.54 HF / 7.52 H_2O. The

gels were transferred to Teflon-lined stainless steel autoclaves and heated at 140 ^{o}C for 25 days. The solids were recovered by filtration, extensively washed with water, and dried at 373 K overnight. The solids were calcined at 580 ^{o}C for 6 h to remove the organic content located in the crystalline material. X-ray diffraction confirmed that the solid materials have the Beta zeolite topology (see Figure S5 for the diffraction pattern of CH_3-Sn-Beta), and SEM EDS measurements for the Sn-Beta, ^{119}Sn-Beta and CH_3-Sn-Beta samples show a Si:Sn atomic ratio of 125:1, 125:1, and 150:1, respectively.

2. Isomerization reactions

Isomerization experiments were carried out in 10 ml thick-walled glass reactors (VWR) heated in a temperature-controlled oil bath placed on top of a digital stirring hotplate (Fisher Scientific). In a typical experiment, 1.5 g of an aqueous solution composed of 10 wt% glucose and the corresponding catalyst amount to achieve a 1:100 metal:glucose molar ratio were added to the reactor and sealed. The reactor was placed in the oil bath and removed at specific times. The reaction was stopped by cooling the reactor in an ice bath, and small aliquots were taken for analysis. Sample analyses were performed by means of high performance liquid chromatography (HPLC) using an Agilent 1200 system (Agilent Technologies Corp.) equipped with PDA UV (320 nm) and evaporative light-scattering (ELS) detectors. Glucose and fructose concentrations were monitored with a Biorad Aminex HPX87C (300 x 7.8 mm) column (Phenomenex), using ultrapure water (pH = 7) as the mobile phase at a flow rate of 0.60 ml/min and a column temperature of 80 ^{o}C.

3. Adsorption experiments

Sn-BEA or Si-BEA catalyst was mixed with 10 wt% of C13-sugar (glucose or fructose) solution at Sn or Si to sugar (glucose or fructose) molar ratio of 1/100 for two hours at room temperature. The mixture was then centrifuged to separate the solid catalyst from the extra glucose solution. Leftover water was removed by leaving the vessel containing the catalyst open overnight in the hood.

4. Characterization

Powder X-ray diffraction (XRD) patterns were collected by using a Scintag XDS 2000 diffractometer using Cu Kα radiation. Scanning electron microscopy (SEM) with Energy Dispersive X-ray Spectroscopy (EDS) measurements were recorded on a LEO 1550 VP FE SEM at an electron high tension (EHT) of 10 kV. UV-Vis measurements were recorded using a Cary 3G spectrophotometer equipped with a diffuse reflectance cell. IR spectra were recorded on a Nicolet Nexus 470 FTIR using a MCT detector. The samples were pressed pellets of pure powder.

Solid-state, magic angle spinning nuclear magnetic resonance (MAS-NMR) measurements were performed using a Bruker Avance 500MHz spectrometer equipped with a 11.7 T magnet and a Bruker 4mm MAS probe. Samples about 60-80 mg in powder were packed into 4mm ZrO_2 rotors and spun at 14 kHz for MAS

experiments. MAS-NMR experiments were conducted for ^{1}H, ^{13}C, ^{23}Na, and ^{119}Sn nuclei of which operating frequencies are 500.2, 125.5, 132.3, 186.5 MHz, respectively. ^{119}Sn MAS NMR spectra were obtained with a recycle delay time of 2 s or 200 s for dehydrated samples. ^{119}Sn cross polarization (CP) MAS spectra were acquired at spinning rate of 10 kHz and using radio frequency (rf) field strength of 62.6 kHz for contact pulse after 4 μsec-π/2 pulse on the ^{1}H channel and strong ^{1}H decoupling during the acquisition. ^{13}C CPMAS experiments were carried out at similar rf field strength. NMR spectra (in ppm) are reported with referenced to tetramethylsilane (TMS) for ^{1}H and ^{13}C, 1M aqueous solution of $Na(NO_3)_3$ for ^{23}Na, and $(CH_3)_3Sn$ but measured with SnO_2 at -604.3 ppm as a second external reference for ^{119}Sn nuclei. For the determination of the amount of the ring-opened carbonyl carbon, the signal intensity of 214 ppm peak in a ^{13}C MAS spectrum of a fructose/Sn-Beta sample was compared with that of ^{13}C MAS spectrum of a known amount of ^{13}C enriched fructose. Once the nuclear spin number of the carbonyl carbon was determined, the number was compared to the number of Sn sites in the sample. For the calculation of Sn sites, the zeolite was simply considered to be pure SiO_2 and Sn spins were obtained from the Si/Sn ratio. Analogous methods were employed to determine the amount of ring-opened fructose from the glucose/Sn-Beta sample.

UV-Vis measurements were recorded using a Cary 3G spectrophotometer equipped with a diffuse reflectance cell. The results for the Sn-Beta samples show the presence of framework Sn and have been published previously.

Results

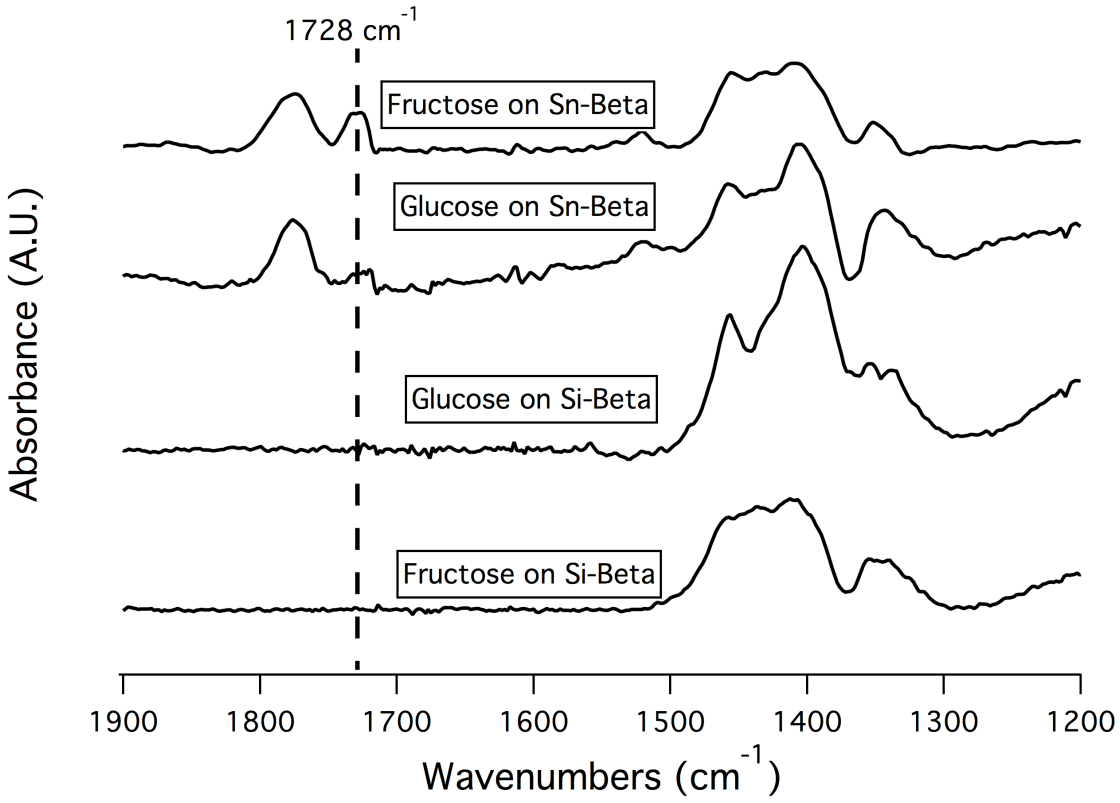

Fig. S1: Infrared spectra of glucose and fructose adsorbed in Sn-Beta and Si-Beta**.** The band at 1775 cm-1 is not assigned to either the ketone or aldedyde groups of the acyclic fructose and glucose, respectively.

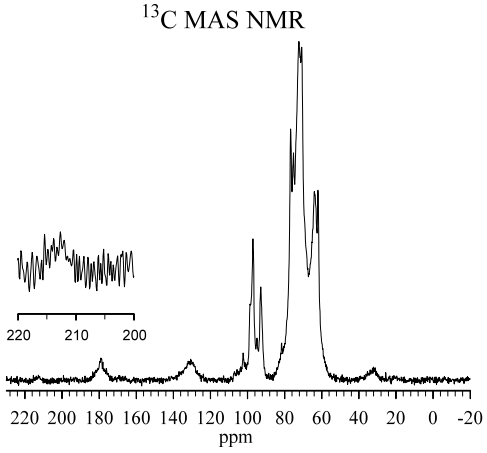

Fig. S2: ^{13}C solid-state NMR spectrum of glucose adsorbed in Sn-Beta.

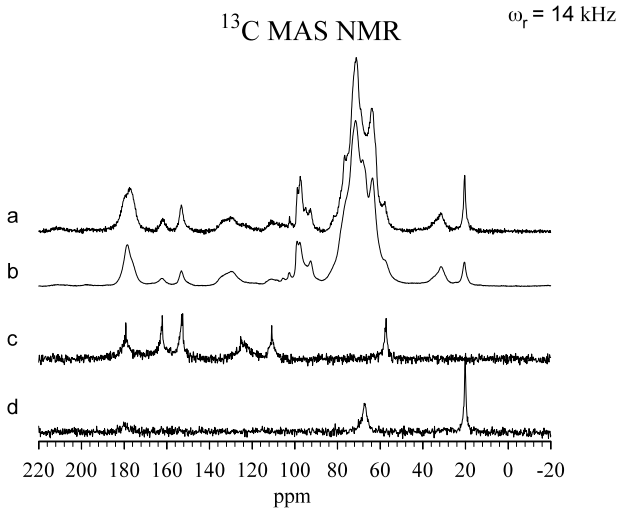

Fig. S3: ^{13}C solid-state NMR of Sn-Beta after reaction conditions using either labeled fructose (a) or labeled glucose (b) as the reactant. Also, HMF absorbed into Sn-Beta (c) and lactic acid absorbed into Si-Beta (d) at room temperature are shown for comparison.

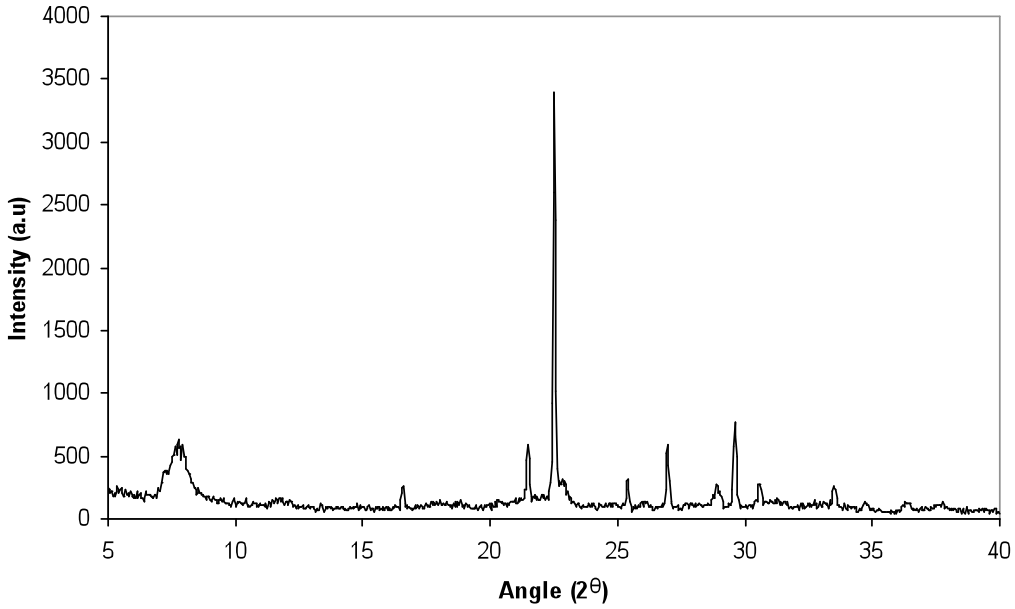

Fig. S4: Powder X-ray diffraction pattern of CH_3Sn-Beta

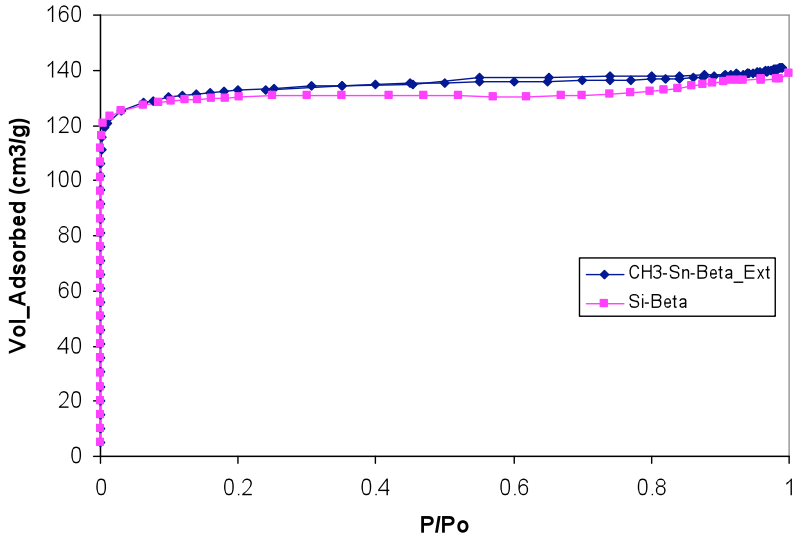

Fig. S5: N_2 adsorption isotherms of Si-Beta and CH_3Sn-Beta extracted.

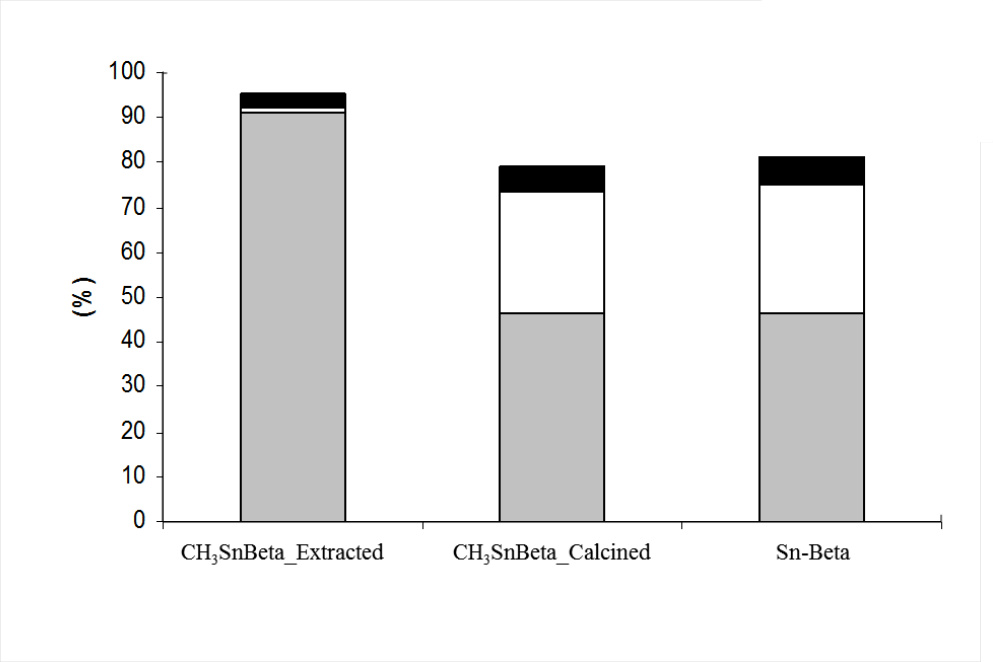

Fig. S6: Glucose isomerization reactivity with Sn-Beta and CH_3Sn-Beta. Grey: Glucose; White: Fructose; Black: Mannose. Reaction conditions: glucose:Sn = 100:1, 110 ^oC, 45 min.

Text S1 Calculation of the kinetic isotope effect.

The kinetic isotope effect is calculated using the expression shown below, derived from transition state theory. The difference in the rate constants between the activation of C-H and C-D bond results mainly for the difference in their zero-point energies (ZPE).

$$\frac{k_H}{k_D} = \exp\left(\frac{ZPE_H - ZPE_D}{kT}\right) = \exp\left(\frac{0.13*h*c*\overline{\nu}_H}{k*T}\right)$$

where $\frac{\overline{\nu}_D}{\overline{\nu}_H} \cong 0.74$, $ZPE = \frac{1}{2}h * c * \overline{\nu}$

h is the Planck's constant with the value of $6.63*10^{34}$ m^2kg/s, c is the speed of light with a value of $2.998*10^8$ m/s, $\overline{\nu}_H$ is the vibrational frequency or wavenumber of a C-H bond scissoring vibration with a value of ~1500 cm^{-1} (we have assumed that the shift of the proton from C2 of glucose to C1 of fructose goes through a bond scissoring vibration), k is the Boltzman constant with a value of $1.38*10^{-23}$ $m^2kg/s^2/K$ and T is the operating temperature in K.

Computational Studies

Text S2 Computational details

The computations in this paper were carried out using the B3LYP(*2*) and the MP2 levels of theory, which is similar to our previous work(*3*) where we reported a detailed mechanism for glyceraldehyde- dihydroxy acetone isomerization by a Sn-beta active site In the computations the Lewis acid metal atom is treated using CC-pVDZ-PP(*4*) , Ahlrich's VTZ(*5*) , 6-31+G(d) basis sets for Sn, Ti, and Si atoms, respectively. The 6-31+G(d) (BS1) basis set is used for the rest of the atoms. The B3LYP level of theory is used for geometry optimization. In order to assess dispersion energies and basis set superposition errors a single point energy evaluation is performed at the MP2 level of theory with a combination of aug-CC-pVQZ (BS2,for Sn(*4*),Ti(*6*),) and 6-311++G(3df,3pd) (rest of the atoms, BS3) on the geometry obtained from the density functional studies. Effective Core Potentials (ECP) for Sn, was used to include relativistic effects in both the DFT and MP2 calculations(*7*). Detailed benchmarking of the theory used in this paper against high level G4(*8*) and CCSD(T) levels of theory are described elsewere(*3*). Frequency calculations were performed to determine whether the stationary points are minima or transition states (TS) and to provide zero point energy corrections (ZPE). Free energy and enthalpy corrections at 298 K were also evaluated using the B3LYP level of theory. In order to account for the effects of aqueous environment, calculations were performed in water dielectric using the SMD solvation model(*9*) at the B3LYP level of theory with the same basis sets as used for the geometry evaluations. In order to evaluate the enthalpy of solvation the non-electrostatic contributions to the solvation energies were excluded. The calculations for this investigation were done using Gaussian 09(*10*)

Text S3: Isomerization catalyzed by Sn-Beta active site models

Information regarding the binding modes of glucose on the Sn-Beta active site is based on the affinity of keto group of the sugar molecule towards the Lewis acid sites and the active involvement of the hydroxyl group (Lewis base) in the open site, which acts as a Lewis base. It has been suggested that the actual active site of Sn-Beta is the $(SiO)_3Sn(OH)$ center and previous density functional studies were reported using this model to understand the energetics and mechanism of the Meerwein-Ponndroff-Verley-Oppenauer reactions (MPVO) between cyclohexanone and 2-butanol(*11*). A recent density functional study also provided insight into the possible role of hydrolyzed T-9 active site of Sn-Beta (Scheme S1 (a) in catalyzing the hydride-shift during the isomerization of aldose to ketose.

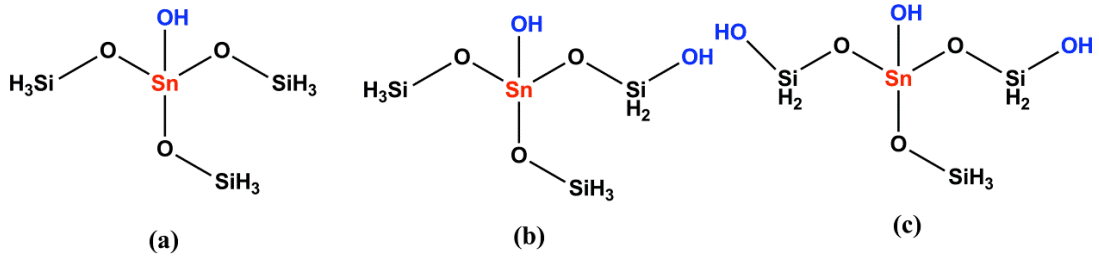

Scheme S1: Schematic representation of the T-9 site of Sn-Beta models used in the computational study: (a) hydrolyzed model, (b) hydrolyzed model with an adjacent single silanol group; and (c) hydrolyzed model with two silanol groups

In aqueous media, the solvation effects of glucose are relatively larger compared to that of a confined space such as in a zeolite pore. In addition to the solvent effect, binding of glucose would be also be affected by the dispersive interaction from the zeolite pore. Therefore, we have incorporated the solvation effect throughout the calculations for determining the free energy and enthalpy profile, and used MP2 level calculations. Thermodynamically, the most favorable binding is through a ring oxygen and an adjacent hydroxyl oxygen ion (C_1-OH, after deprotonation) coordinates to the metal center in aqueous environments. This model provides insight to the reaction barrier for the ring opening mechanism with the participation of basic hydroxyl group in the presence of the central metal atom. An alternative binding mode of glucose would be through its hydroxyl groups to the metal center; however, the free energy of this interaction is thermodynamically uphill both in gas phase and in aqueous environment. Binding through the ring oxygen and the hydroxyl group at C1 position was computed as thermodynamically more favorable compared to any two hydroxyl groups of glucose. Therefore, this was considered as the initial binding mode of glucose to the active site in this study. From this binding mode, we have proposed a mechanism, which involves the ring opening, hydride shift, ring closing and computed a detailed free energy profile at the MP2 levels of theory in a water dielectric (298 K) for the conversion of glucose to fructose by the Sn-active site model. The computed free energy profile is shown in Figure S7 and the enthalpy profile is shown Figure S8. All energies are relative to the initial state **A**, the sum of the isolated Sn-$(OSiH_3)_3$-OH active site and glucose in aqueous dielectric at infinite distance. The interaction of cyclic glucose with the active site model (Scheme S1, (a)) to form the initial complex (**I**) is thermodynamically downhill and highly exothermic (-17.1 kcal/mol) in aqueous media. The Gibbs free energy of complexation is quantitatively smaller than the change in enthalpy in solution due to the decrease in entropy upon binding to the active site. Additionally, the free energy of complexation in solution is quantitatively smaller than the gas phase due to the decrease in solvation energy of hydrophilic glucose upon complexation. The hydroxyl group (Lewis base) of the active site picks up a proton from the C_1-OH and forms a water molecule and an open chain aldehyde (II). This process (proton transfer) requires a Gibbs free energy barrier of 10.6 kcal/mol (3.3 kcal/mol in gas phase) and results in the formation of a strong Sn-O_{ring} bond of 2.04 Å and weak Sn----OH_2(2.33 Å) bond. The cleavage of the Sn-O_{ring} bond occurs through the protonation of oxygen by the water ligand resulting in the formation of acyclic glucose weakly coordinated with the catalytic center (III).

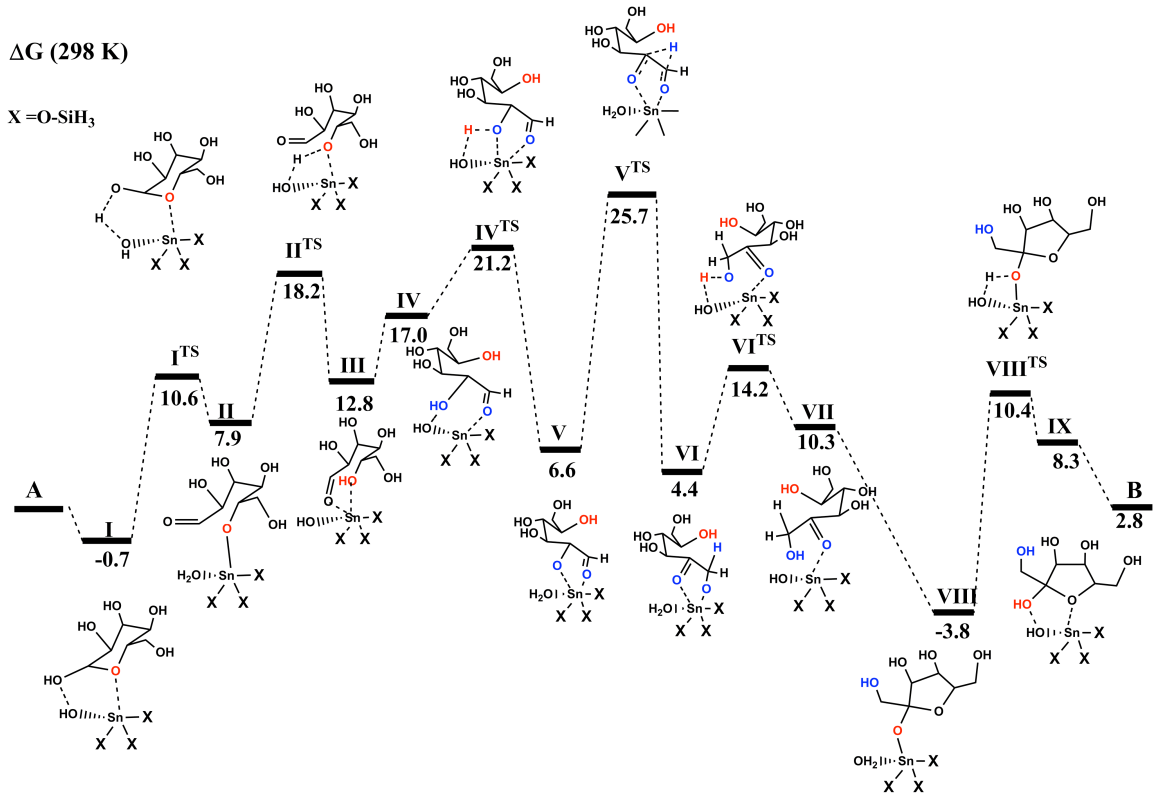

Fig. S7: The computed Gibbs free energy landscape of the isomerization of glucose-fructose catalyzed by the Sn-$(OSiH_3)_3$-OH active site model at the MP2 level of theory in an aqueous dielectric medium. The aqueous effects were modeled using the SMD solvation model at 298 K. The label A denotes the sum of Gibbs free energy of glucose and active site model (a) (Scheme 1) infinitely separated in aqueous medium, the B denotes the same quantity for fructose. All energies are in kcal/mol.

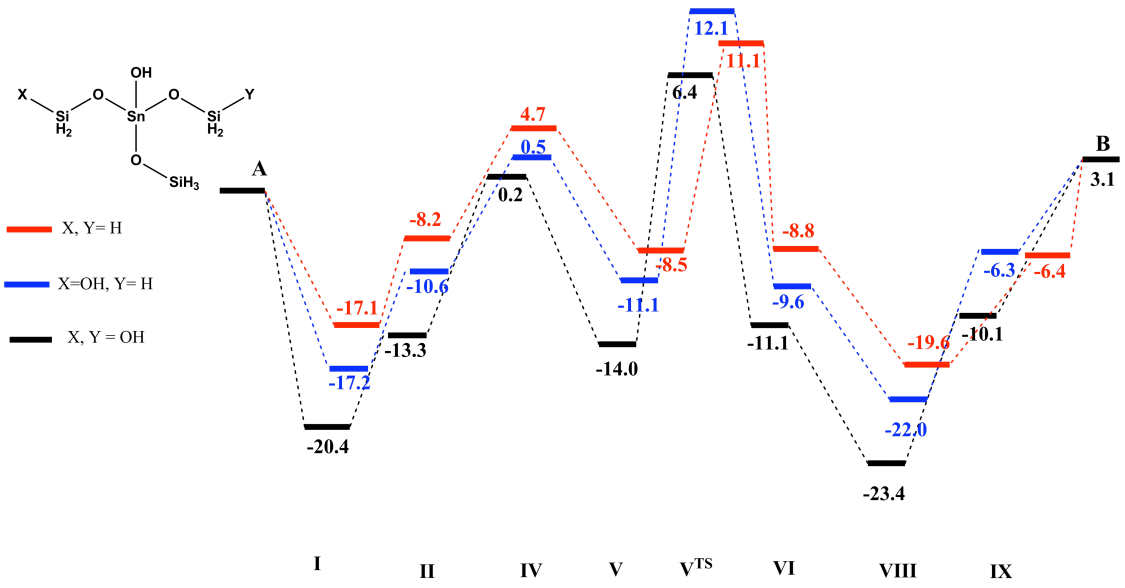

Fig. S8: The computed enthalpy profile (MP2, at 298 K in water dielectric) for glucose-fructose isomerization catalyzed by different open sites of Sn-Beta. The reaction coordinates are given in the X-axis. The label A denotes the sum of enthalpy of glucose and active site models infinitely separated in aqueous medium, B denotes the same quantity for fructose. All energies are relative to the energy of A and reported in kcal/mol.

This process requires an activation free energy of 18.2 kcal/mol (II^{TS}) and this process (II to III) of partially detaching acyclic glucose from the active site is thermodynamically uphill (4.9 kcal/mol). Binding of acyclic glucose to the Sn-active site is much weaker than cyclic glucose and moderately uphill compared to the free energy of the initial state **A** in aqueous solution. Deprotonation of the hydroxyl group at the C_2 position by the Lewis base requires an apparent activation free energy barrier of 21.2 kcal/mol and the computed true barrier ($IV \rightarrow IV^{TS}$) for this proton transfer is 4.2 kcal/mol. This process (IV to V) is thermodynamically downhill (by 11.0 kcal/mol) due to formation of a Sn-O bond and water. This process is followed by the hydride shift from the C2 to C1 carbon atom (**V** to **VI**). The hydride shift occurs through a hexa-membered transition state and requires an apparent activation free energy barrier of 25.7 kcal/mol with the active participation of a tin atom by activation of the keto oxygen atoms of the sugar molecule. The true activation free energy barrier for ($V \rightarrow V^{TS}$) is 19.1 kcal/mol and the true activation enthalpic barrier for this reaction is 19.6 kcal/mol. Also note that, the apparent activation enthalpy barrier for this reaction is 11.1 kcal/mol in aqueous solution and the hydride shift (V→VI) is a thermodynamically downhill process. The hydride shift is followed by the transfer of a proton from the water ligand to the oxygen attached to the C1 carbon (VI to VII) and then ring closure (VII to VIII). The first process occurs through the deprotonation of a water ligand and the resulting hydroxyl group transforms back to water through re-protonation from the hydroxyl group attached to the C_6 carbon atom. The activation free energy barrier for the reaction VI to VII is 14.2 kcal/mol. The ring closure ($VIII^{TS}$) from the intermediate (VIII) is calculated to be barrier-less in aqueous solution due to the relative stabilization from aqueous dielectric for the cyclic fructo-furanose form. The complex formed (VIII) after the ring closure is

thermodynamically stable and has a relative free energy of -3.8 kcal/mol in aqueous solution. A proton transfer (activation free energy barrier of 10.4 kcal/mol) from water ligand to the oxygen atom cleaves the Sn-O bond forming, the intermediate IX. This intermediate is 8.3 kcal/mol higher in free energy than **A**. The separated cyclic fructose and the active site model (B) that form from IX have an energy of 2.8 kcal/mol relative to A. The highest point in the free energy profile is the hydride shift, which is assumed to be the rate-limiting step. This is consistent with the recently published experimental studies(*12, 13*)

Text S4 Calculation of Apparent activation enthalpy

The apparent enthalpy was obtained by performing a micro-kinetic analysis using the elementary steps in enthalpy profiles (Sn-Beta: Figure S8, Ti-Beta : Figure S10, vide infra) for each of the active sites. The 1,2-hydride shift was assumed to be the rate limiting step. The apparent activation enthalpy can be calculated using the following equation,

$$H^{act}_{apparent} = H^{act}_{true} + \Delta H^{adsorption},$$

where $H^{act}_{apparent}$, H^{act}_{true}, and $\Delta H^{adsorption}$ are apparent activation enthalpy, true barrier (hydride shift), and change in enthalpy of adsorption of the most abundant intermediates (exothermic adsorption), respectively.

The $\Delta H^{adsorption} = \Sigma \Delta H^{reactant\ intermediates} - \Sigma \Delta H^{product\ intermediates}$. Using the above expression, the apparent activation enthalpies for the glucose-fructose isomerization catalyzed by Sn-Beta active site models (a, b, c in Scheme S1) were computed and shown in Table S1.

Table S1: Computed true activation enthalpy (H^{act}_{true}), change in adsorption enthalpy ($\Delta H^{adsorption}$) and apparent enthalpy of activation ($H^{act}_{apparent}$) for glucose-fructose isomerization catalyzed by active site models for Sn-Beta (Scheme S1: a, b, c) and Ti (Scheme S2: d, e, f). The energy evaluated at the MP2 level of theory. The calculations are performed at 298 K, and contribution to enthalpies from aqueous dielectric is also included. All energies are reported in kcal/mol**.**

active site model	H^{act}_{true}	$\Delta H^{adsorption}$	$H^{act}_{apparent}$
(a)	19.6	-1.0	18.6
(b)	23.2	-1.1	22.1
(c)	20.6	-3.3	17.3
(d)	20.2	+7.8	28.0
(e)	20.2	+14.1	34.3
(f)	17.6	+18.8	36.4

The computed activation enthalpies for glucose to fructose isomerization catalyzed by active site models a, b, and c (Scheme S1) are 18.6, 22.1, and 17.3 kcal/mol respectively. The computed activation enthalpy of active site model b (22.1 kcal/mol), Sn-Beta active site with one adjacent Si-OH group is consistent with the experimental activation energy of 21.2 kcal/mol from our experimental kinetic studies. These results suggest that the active site for the Sn Beta, which promotes the isomerization process, is in fact a hydrolyzed site rather than the close site. Previously it was shown that, the apparent activation energy for the hydride shift associated with the isomerization of glyceraldehyde to dihydroxy acetone is 10 kcal/mol higher for the closed site than the open site.(*3*)

Text S5 Isomerization catalyzed by Sn-Beta Closed Site model.

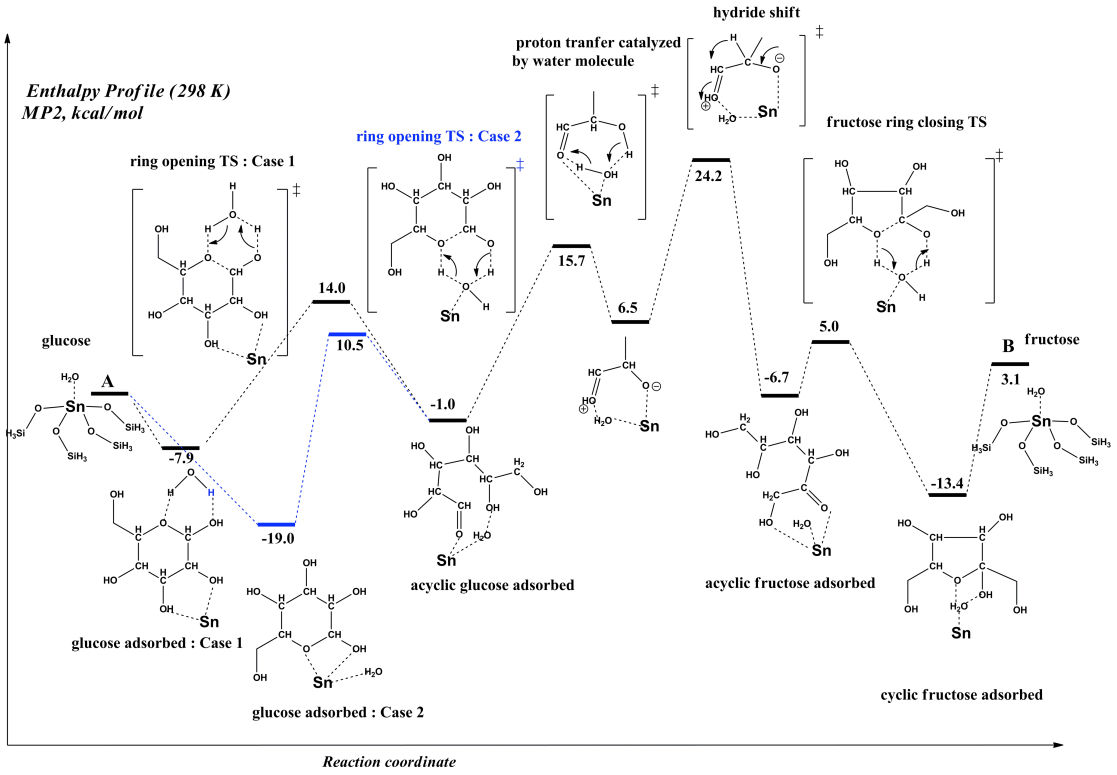

Fig. S9: The computed enthalpy profile of the isomerization of glucose-fructose catalyzed by the Sn-$(OSiH_3)_4$- H_2O active site model at the MP2 level of theory in an aqueous dielectric medium. The aqueous effects were modeled using the SMD solvation model at 298 K. The label A denotes the sum of Gibbs free energy of glucose and active site model (Sn-$(OSiH_3)_4$- H_2O) infinitely separated in aqueous medium, the B denotes the same quantity for fructose. All energies are reported in kcal/mol**.**

The detailed enthalpy profile for the glucose-fructose isomerization catalyzed by Sn-Beta closed site (**Sn-$(OSiH_3)_4$- H_2O)** is shown in Figure S9. Due to the lack of a Lewis base in the closed site model the ring opening and closure is catalyzed by water which is coordinated with Sn site. Different modes of cyclic glucose adsorption were considered. Our calculations suggest that upon strong adsorption of glucose (Case 2 in Figure S9), the rate-limiting step is the ring opening of glucose, while for weaker absorption the rate-limiting step is the hydride shift. Based on the micro-kinetic model, the computed apparent activation enthalpy is 30 kcal/mol regardless of the initial adsorption. These calculations suggest that the closed site can also catalyze the isomerization process, but not a primary catalytic site due to requirement of a relatively larger activation enthalpy compared to the open site. Another important observation is the relative stability of complex formed upon adsorption of acyclic fructose with closed site compared to open site.

Text S6 Isomerization catalyzed by Ti-Beta active site models

We have also utilized MP2 theory to calculate the energy associated with elementary steps involved in the isomerization of acyclic glucose to fructose on a number of different Ti-Beta active site models including: (d) an open site where framework Ti is bound in one direction with an OH group and in the other three directions with framework Si through bridging oxygen atoms , (e) an open site as in (f) with an one adjacent silanol (Si-OH) group, and an open site as in (d) with two adjacent silanol (Si-OH) groups (Scheme S2) We found that the lowest energy pathway for the isomerization of acyclic glucose to fructose on all the Ti-Beta active sites involves a hydride shift from the second carbon (C2) in acyclic glucose to the first carbon (C1) in fructose as the rate-limiting step, similar to open site of Sn-Beta (Figure S7). Here, we have computed the detailed enthalpy profile for glucose-fructose isomerization catalyzed by all these sites (Figures S9 and S10) for comparison with the experiments and with the Sn-Beta results.

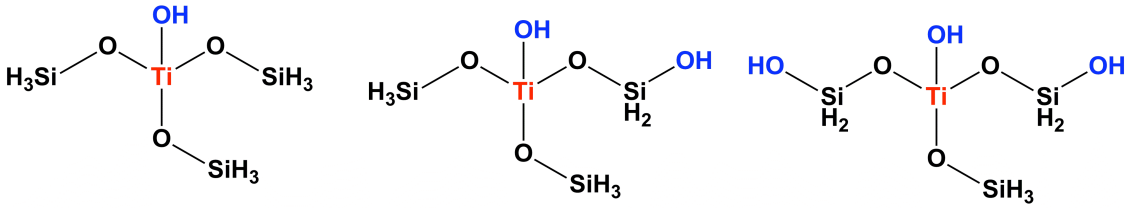

Scheme S2: Schematic of different Ti-Beta active sites used in the computational models. d) open Ti site, e) open Ti site with one Si-OH group and f) open Ti site with two Si-OH group**.**

Figure S10 presents a comparison of the enthalpy profile for the glucose-fructose isomerization by open site of Sn-Beta (with one silanol) and Ti-Beta (with one silanol group). The computed rate limiting step and the initial enthalpy of binding of glucose suggests that Sn-Beta is a much superior catalyst for the isomerization than the Ti-Beta. This is consistent with the reported studies. Figure S11 shows the calculated energetics (enthalpies) associated with various elementary steps involved in the isomerization of acyclic glucose to fructose on the three different active sites. We found that for all three models of the active site (d, e, f), the rate limiting step is the 1,2 hydride shift. The computed apparent activation energies for glucose-fructose isomerization catalyzed by Ti-Beta active site models (d,e,f) is given in Table S1.

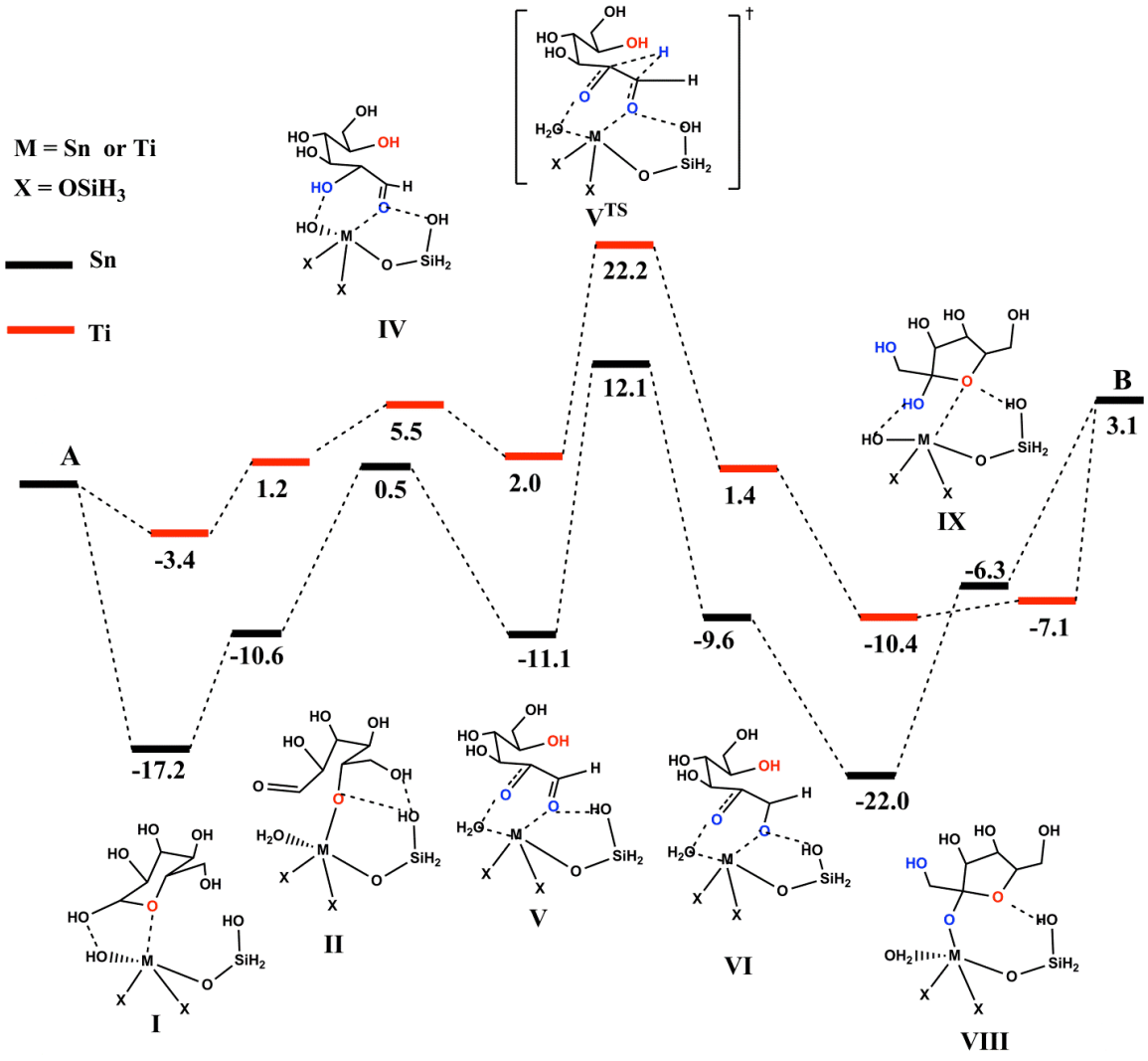

Fig. S10: Comparison of the enthalpic profile of the open site of Sn-Beta and Ti-Beta for the glucose-fructose isomerization. The MP2 level of theory is employed to compute the enthalpy surface. The solvation contribution in the enthalpy is computed using the SMD solvation model. The label A denotes the sum of enthalpy of glucose and active site model (b and e) infinitely separated in aqueous medium, the B denotes the same quantity for fructose. All energies are reported in kcal/mol.

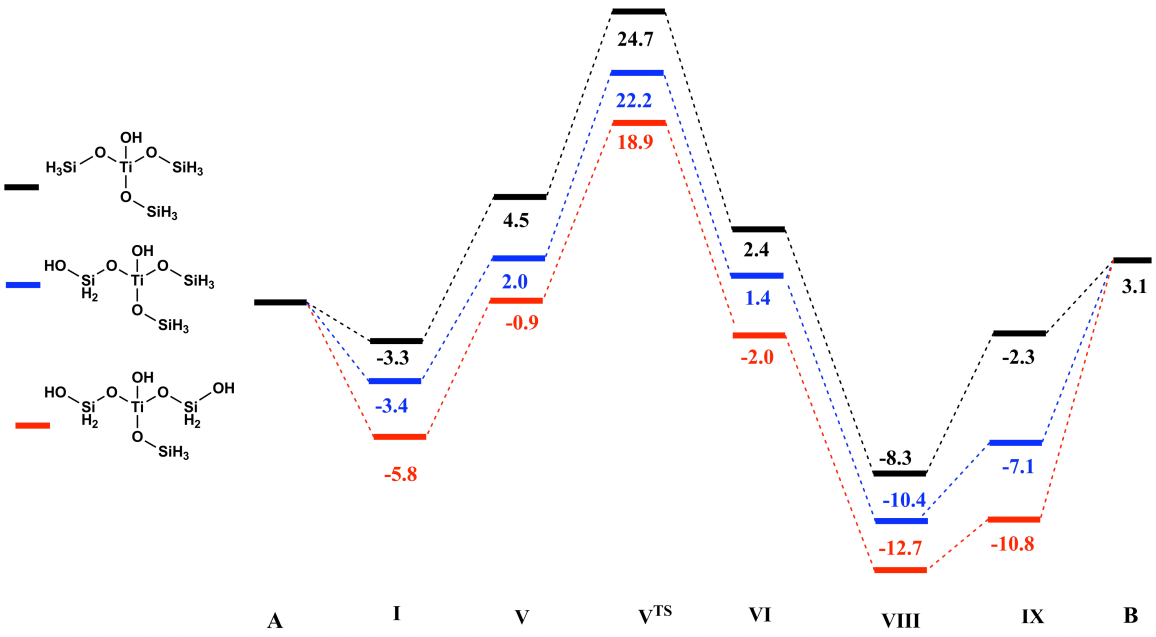

Fig. S11: Enthalpy profile (MP2) for the glucose-fructose isomerization by different Ti-Beta active site models. The X-axis denotes the reaction coordinate. See Figure S9 for the schematic representation for species II to IX. The label A denotes the sum of enthalpy of glucose and active site model (d,e,f) infinitely separated in aqueous medium, the B denotes the same quantity for fructose. All energies are reported in kcal/mol.

The computed apparent enthalpy for the glucose-fructose isomerization catalyzed by models d, e, and f (Scheme S2) are 28.0, 34.3 and 36.3 kcal/mol respectively. If we compare our calculated overall activation barriers with the measured barriers we find that our measured activation enthalpy (37.1 kcal/mol) is very similar to the one calculated for the Ti open site with one and two silanol group model system (34.3 & 36.3 kcal/mol). Since the apparent activation barriers for the open Ti site with one and two adjacent silanol group are very close in energy, it would be difficult to distinguish between these two sites based on the MP2 calculations. Therefore, we can only conclude based on comparing the MP2 calculations with the experimental data that the active site in Ti-Beta is a form of an open Ti site, which involves a hydrated Ti-OH center with adjacent silanol groups.

References:

1. M. Tamarasso, G. Perego, B. Notari. (U.S Pat. 4,410,501, 1983).
2. A. D. Becke, Density-Functional Thermochemistry .3. The Role of Exact Exchange. *J. Chem. Phys.* **98**, 5648 (1993).
3. R. S. Assary, L. A. Curtiss, Theoretical Study of 1,2-Hydride Shift Associated with the Isomerization of Glyceraldehyde to Dihydroxy Acetone by Lewis Acid Active Site Models. *J. Phys. Chem. A* **115**, 8754 (2011).

4. K. A. Peterson, Systematically convergent basis sets with relativistic pseudopotentials. I. Correlation consistent basis sets for the post-d group 13-15 elements. *J. Chem. Phys.* **119**, 11099 (2003).
5. A. Schafer, H. Horn, R. Ahlrichs, Fully Optimized Contracted Gaussian-Basis Sets for Atoms Li to Kr. *J. Chem. Phys.* **97**, 2571 (1992).
6. N. B. Balabanov, K. A. Peterson, Systematically convergent basis sets for transition metals. I. All-electron correlation consistent basis sets for the 3d elements Sc-Zn. *J. Chem. Phys.* **123**, (2005).
7. P. J. Hay, W. R. Wadt, Abinitio Effective Core Potentials for Molecular Calculations - Potentials for the Transition-Metal Atoms Sc to Hg. *J. Chem. Phys.* **82**, 270 (1985).
8. L. A. Curtiss, P. C. Redfern, K. Raghavachari, Gaussian-4 theory. *J. Chem. Phys.* **126**, 084108 (2007).
9. A. V. Marenich, C. J. Cramer, D. G. Truhlar, Universal Solvation Model Based on Solute Electron Density and on a Continuum Model of the Solvent Defined by the Bulk Dielectric Constant and Atomic Surface Tensions. *J. Phys. Chem. B* **113**, 6378 (2009).
10. Gaussian 09, M. J. Frisch, G. W. Trucks, H. B. Schlegel, G. E. Scuseria, M. A. Robb, J. R. Cheeseman, G. Scalmani, V. Barone, B. Mennucci, G. A. Petersson, H. Nakatsuji, M. Caricato, X. Li, H. P. Hratchian, A. F. Izmaylov, J. Bloino, G. Zheng, J. L. Sonnenberg, M. Hada, M. Ehara, K. Toyota, R. Fukuda, J. Hasegawa, M. Ishida, T. Nakajima, Y. Honda, O. Kitao, H. Nakai, T. Vreven, J. A. Montgomery, Jr., J. E. Peralta, F. Ogliaro, M. Bearpark, J. J. Heyd, E. Brothers, K. N. Kudin, V. N. Staroverov, R. Kobayashi, J. Normand, K. Raghavachari, A. Rendell, J. C. Burant, S. S. Iyengar, J. Tomasi, M. Cossi, N. Rega, J. M. Millam, M. Klene, J. E. Knox, J. B. Cross, V. Bakken, C. Adamo, J. Jaramillo, R. Gomperts, R. E. Stratmann, O. Yazyev, A. J. Austin, R. Cammi, C. Pomelli, J. W. Ochterski, R. L. Martin, K. Morokuma, V. G. Zakrzewski, G. A. Voth, P. Salvador, J. J. Dannenberg, S. Dapprich, A. D. Daniels, Ö. Farkas, J. B. Foresman, J. V. Ortiz, J. Cioslowski, and D. J. Fox, Gaussian, Inc., Wallingford CT, 2009.
11. M. Boronat, A. Corma, M. Renz, Mechanism of the Meerwein-Ponndorf-Verley-Oppenauer (MPVO) Redox Equilibrium on Sn- and Z-Beta Zeolite Catalysts. *J. Phys. Chem. B* **110**, 21168 (2006).
12. M. Moliner, Y. Román-Leshkov, M. E. Davis, Tin-containing zeolites are highly active catalysts for the isomerization of glucose in water. *Proc. Nat. Acad. Sci.* **107**, 6164 (2010).
13. Y. Román-Leshkov, M. Moliner, J. A. Labinger, M. E. Davis, Mechanism of Glucose Isomerization Using a Solid Lewis Acid Catalyst in Water. *Angew. Chem. Int. Ed.* **49**, 8954 (2010).